Supporting Information

Protein-Rich Marine Spirulina for Synthesizing Biocompatible Carbon Dots with High Quantum Yield for Fluorescent yarns

Lihui Hou [a], Tianyi Xin [a], Weihua Li [a], Tao Zhao [a], Yuanming Zhang [a], Haiguang Zhao [a, *], Wei Jiang [a, *], Yi Han [a, *]

[a] College of Life Sciences and College of Textiles & Clothing, Qingdao University, Qingdao 266071, China

*Corresponding author.

hgzhao@qdu.edu.cn (H. Zhao); weijiangqd@qdu.edu.cn (W. Jiang); hanyiqdu@qdu.edu.cn (Y. Han).

1. Characterizations

The morphologies and structures of the as-prepared C-dots were measured by transmission electron microscope (TEM, JEOL 2100 F, Japan). The morphology of the spun yarns was characterized using a scanning electron microscope scanning (SEM, JSM-6390LV, Japan). Fourier transform infrared spectrometer (FT-IR, Nicolet 6700, USA) and X-ray photoelectron spectrometer (XPS, AXIS Supra, Japan) were used to characterize the surface chemical structure of C-dots. The absorption property of the C-dots was characterized by a UV-visible spectrophotometer (UV-2600, Japan); the fluorescence spectrum, fluorescence lifetime and QY of the purified C-dots were characterized by steady state/transient fluorescence spectrometer (FLS1000, Britain), assisted with an integration sphere. Zeta potential was measured on a Malvern Zetasizer Nano ZSE (DLS-Zeta potential, Britain). Magnetic stirrers were employed to ensure homogeneous mixing of the solutions. Electrospun yarns were fabricated using an electrospinning apparatus (HZ-SX-01).

2. HPLC Conditions

Chromatographic column Bio-Rad Aminex HPX-87 H, eluent 0.002 mol/L H_2SO_4, flow rate 0.6 mL/min, column temperature 50 ℃, injection volume 10 μL, and a differential refractive index detector (RID, 45 ℃).

3. Chemical Profiling of *Spirulina*

A total of 300.0 ± 10.0 mg of algal powder was accurately weighed into a beaker, and the exact mass was recorded to the nearest 0.1 mg. Subsequently, 3.00 ± 0.01 mL of 72% (w/w) sulfuric acid was added, and the mixture was stirred thoroughly with a glass rod until fully homogenized. The beaker was then placed in a water bath maintained at 30 ± 3°C for 60 ± 5 min. During this period, the sample was stirred every 5 to 10 min to ensure consistent hydrolysis.

After completion of the hydrolysis, the contents of the beaker were transferred to an Erlenmeyer flask. Then, 84.00 ± 0.04 mL of deionized water was added to dilute the

acid to a final concentration of approximately 4% (w/w). The flask was sealed with aluminum foil and autoclaved at 121°C for 60 min to complete the hydrolysis process. The hydrolyzed *Spirulina* was centrifuged, and the supernatant was filtered (filtration film pore size 0.22 μm), and then tested by HPLC under the same conditions as above.

4. Experimental details for calculating quantum yield

The QYs of the purified C-dots measured by an Edinburgh FLS1000 instrument with a xenon arc lamp and integrated with an integrating sphere. The excitation wavelength was set at 375 nm, and the emission spectrum was recorded over the range of 355-900 nm. The QY was calculated based on the ratio of emitted photons to absorbed photons, following the standard procedure for absolute QY determination. A blank measurement was performed prior to sample analysis to correct for background signals (The blank sample was deionized water). The QY was directly obtained by calculating based on the following equation:

$$\phi = (PL_{Sample} - PL_{Control}) / (E_{Control} - E_{Sample}) \times R$$

Where PL_{sample} and $PL_{Control}$ are the integrated PL area of the sample and the scattering curve, respectively, and $E_{control}$ and E_{sample} are the integrated excitation area of the scattering and the sample curve, respectively. R is the equipment coefficient, which is obtained directly during the measurement by knowing the PL spectrum of the C-dots. In this work, the reported absolute QYs are the sum of fluorescence.

5. Electrospinning Parameters

The feed rate of the TVB precursor was 2.5 mL h^{-1} on both the left and right sides. A positive voltage of 7-10 kV (left side) and a negative voltage of 6-7 kV (right side) were applied. The rotational speed of the horn for collecting TVB fibers was 160-200 rpm, and the speed of the TVB yarn collector was 1 rpm. The ambient temperature and relative humidity were 27 ± 2 ℃ and 50 ± 5%, respectively.

6. Figures

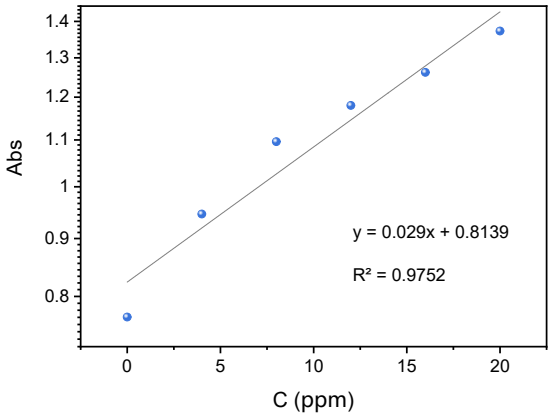

Figure S1. BSA (Bovine Serum Albumin) Calibration curve for Bradford Method.

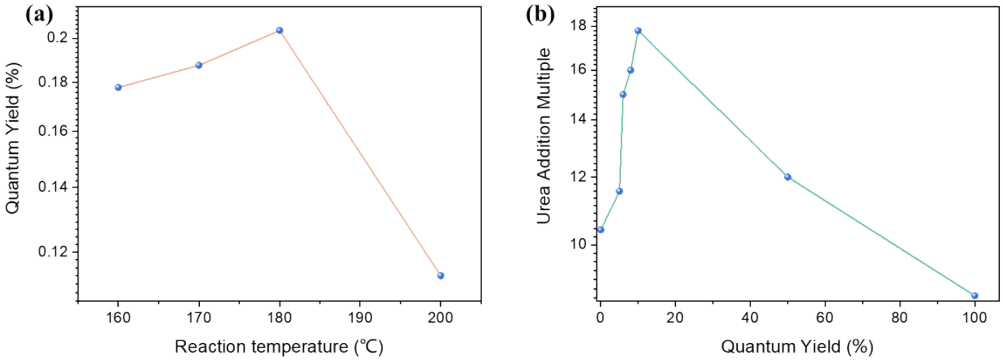

Figure S2. (a) The influence of temperature on the QY of carbon dots. (b) The change of QY of CDs corresponding to urea concentration.

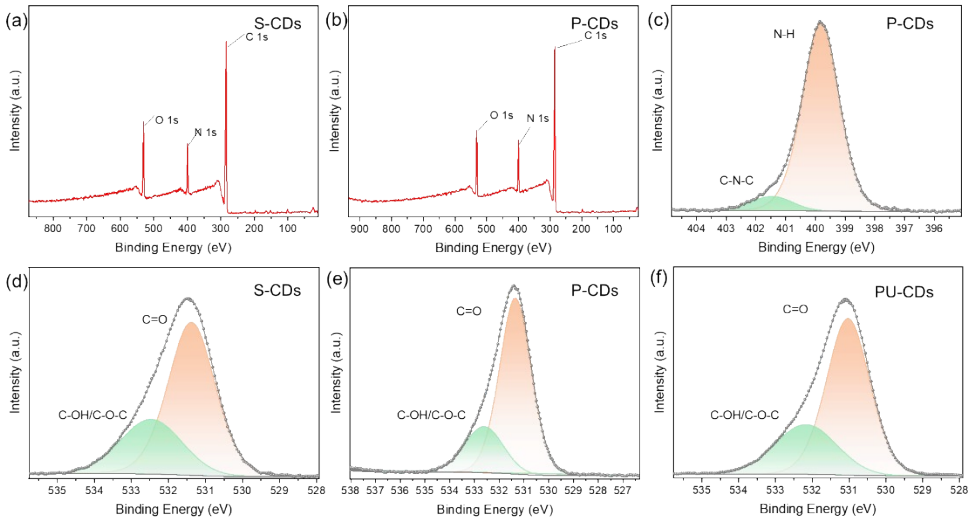

Figure S3. (a) The full survey XPS spectra of the S-CDs. (b) The full survey XPS spectra of the P-CDs. (c) The high-resolution XPS spectra of the N l s of the P-CDs. (d) The high-resolution XPS

spectra of the O l s of the S-CDs. (e) The high-resolution XPS spectra of the O l s of the P-CDs. (f) The high-resolution XPS spectra of the O l s of the PU-CDs.

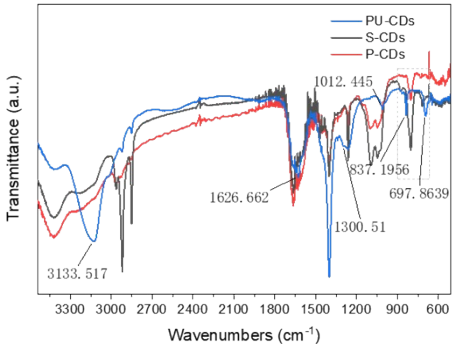

Figure S4. FT-IR spectroscopy of the S-CDs, P-CDs and PU-CDs.

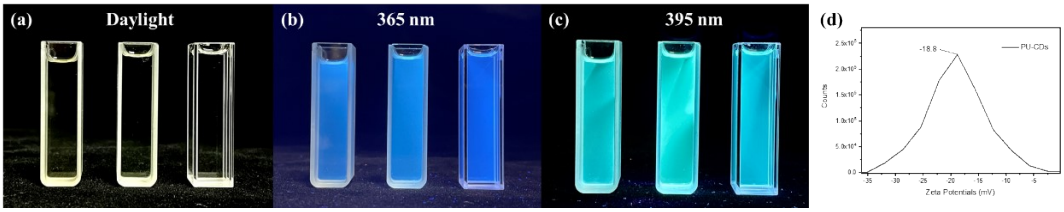

Figure S5. The fluorescence effect of CDs in different environments (samples S-CDs, P-CDs, and PU-CDs in sequence). (d) Zeta potential curve of the PU-CDs.

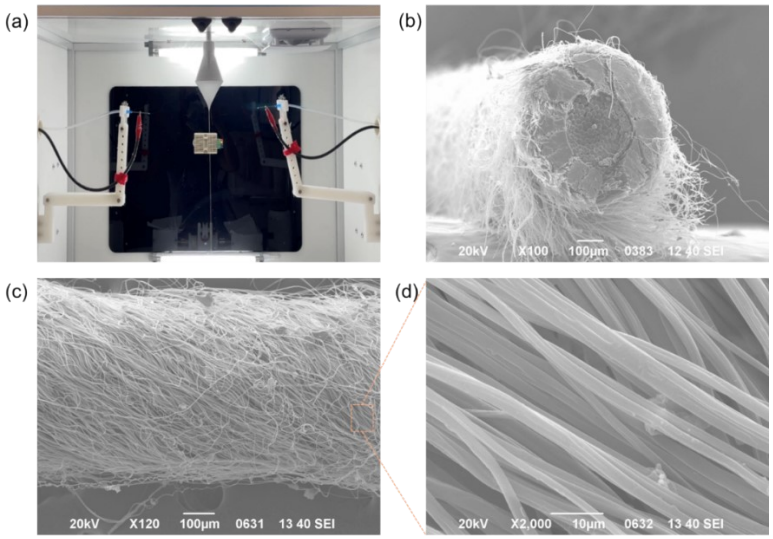

Figure S6. (a) Schematic illustration of the electrospinning apparatus. (b) Cross-sectional SEM image of the E-FYS (c and d) SEM images of E-FYs at different magnifications.

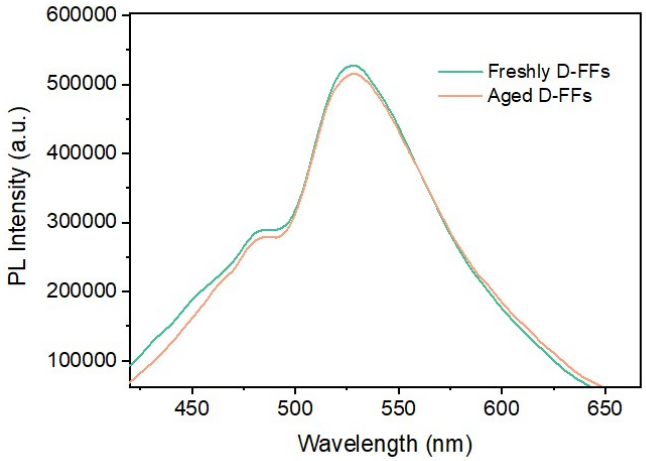

Figure S7. Fluorescence performance of fibers after different storage durations.

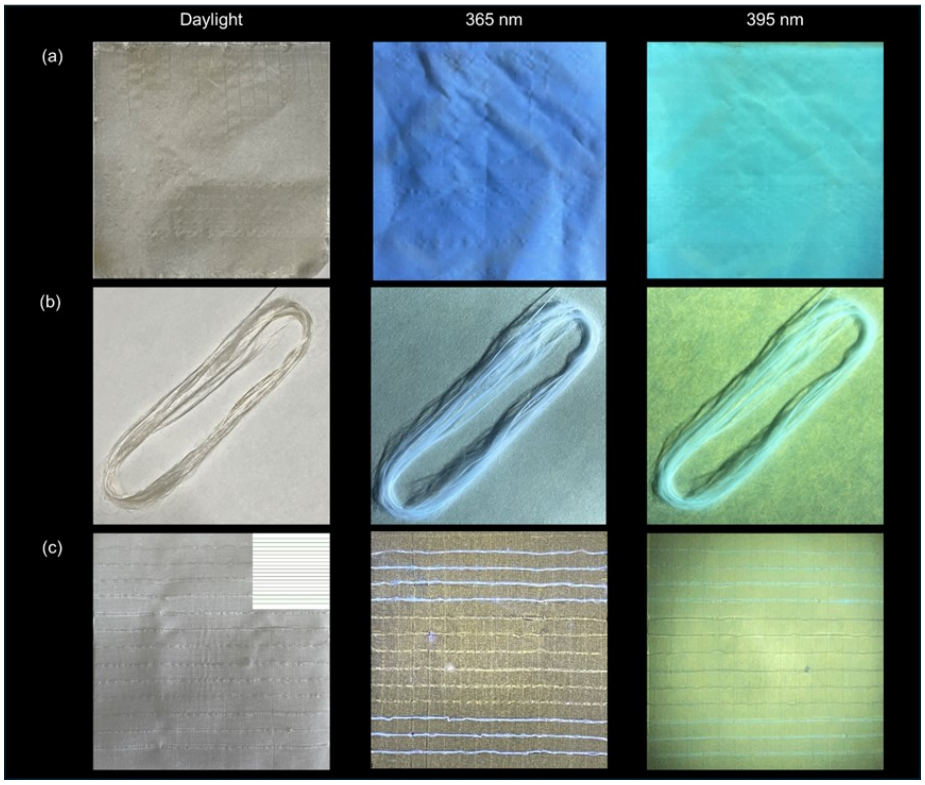

Figure S8. (a) The dyeing effect of the PU-CDs on nylon fabric. (b) The dyeing effect of the PU-CDs on nylon yarn. (c) Simulated weaving effect using fluorescent yarns under different light sources.

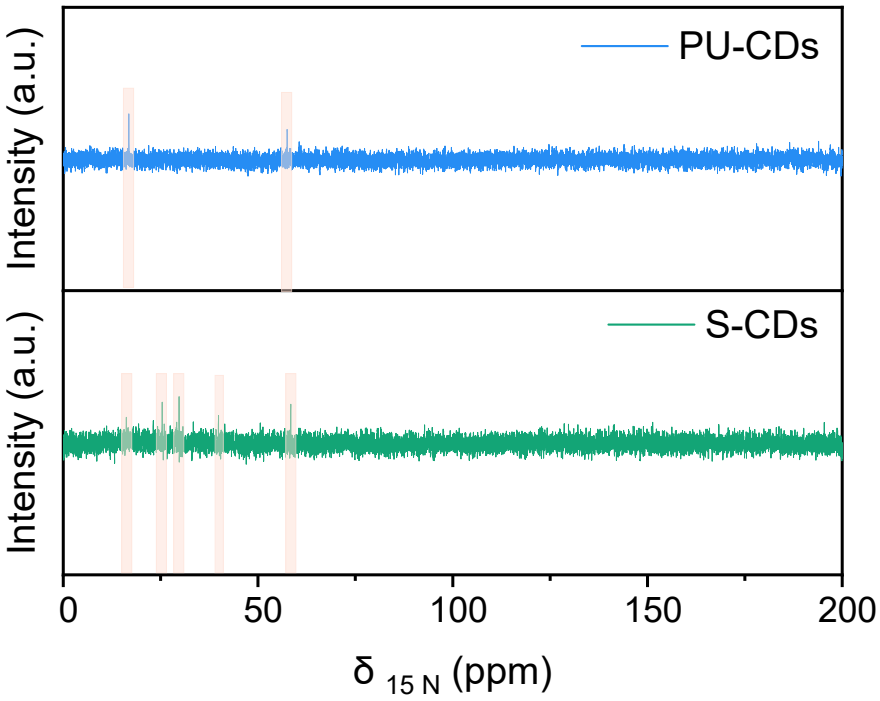

Figure S9. Comparison of solid-state ^{13}C NMR spectra between S-CDs and PU-CDs.

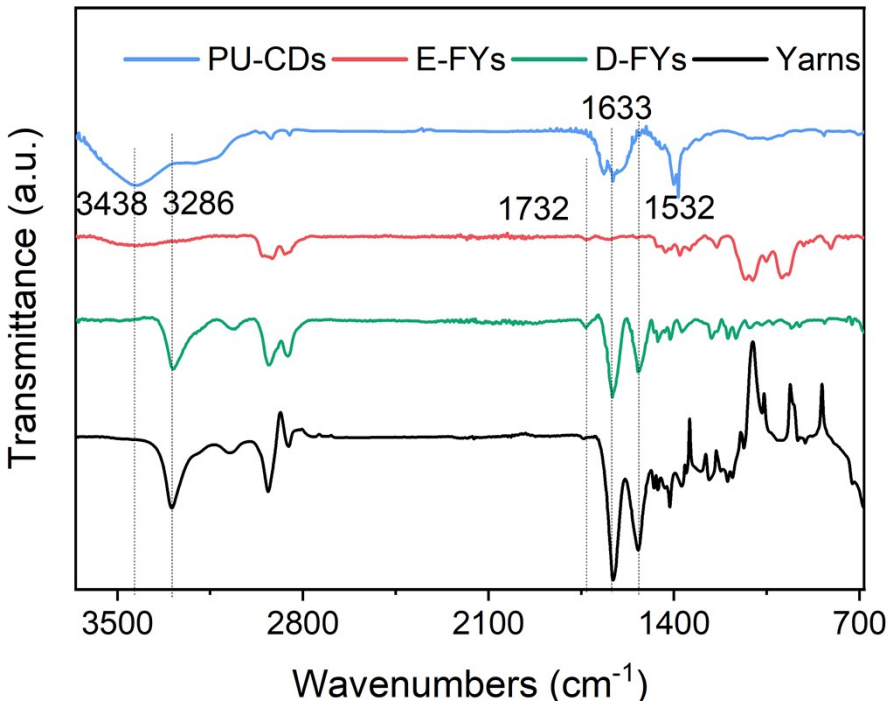

Figure S10. FT-IR spectra of PU-CDs, E-FYs and D-FYs.

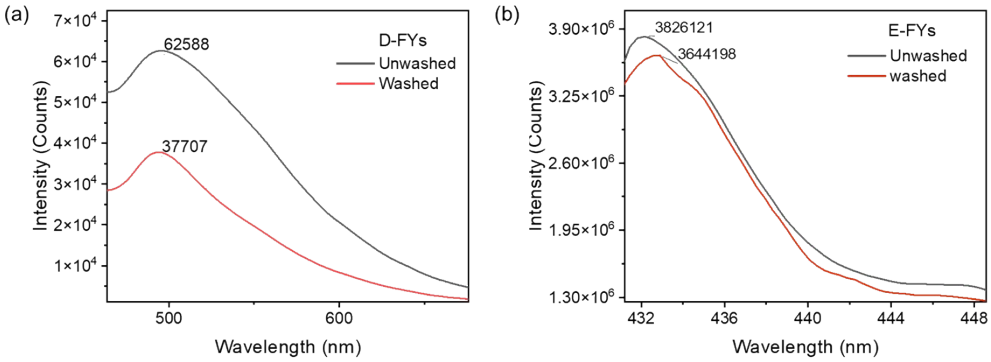

Figure S11. PL intensity changes of (a) D-FYs and (b) E-FYs after each standard washing fastness cycle.

7. Tables

Table S1.

Comparison of fluorescence QY of carbon dots synthesized from various biomass precursors.

Reactant	QY (%)	References
Bee Pollen	2.15 and 4.8	[1]
Watermelon Peel	7.1	[2]
Sarcocarp	8.97	[3]
Avocado Peel	9.56	[3]
Watermelon	0.4	[4]
Sugarcane Bagasse Pulp	18.7	[5]
Banana Peel	20.0	[6]
Nitrogen-doped Grape Peels	15.3	[7]
Mangifera Indica leaves	18.2	[8]
Wedelia Trilobata	18.6	[9]
Pine Needles	16.4	[10]
Lotus Leaves	15.3	[10]
Oriental Plane Leaves	11.8	[10]
Natural Spinach	12.68~30.77	[11]
Litchi Peel	7.20	[12]
Activated Carbon	19.60	[13]
Lentinus Edodes	14.27	[14]
Peach Blossom	26.00	[15]
Balsa Wood	2.82	[16]
Maple Leaves	5.60	[17]
Red Jujube	0.81	[18]
Eucalyptus Wood Chips	19.43	[19]
Pig Bone	26.40	[20]
Gluconic Acid	6.01	[21]
Flue Ash	3.83	[22]

Corn Starch	38.50	[23]
Waste Lignin	12.00	[24]
Commercially Available Tobacco Leaves	4.88	[25]
Biomass Sugarcane Bagasse	14.60	[26]
Peanut Kernel	5.00	[27]

Note reference: The carbon dots synthesized in this study exhibit a quantum yield of 20.4%, indicating a relatively high level of fluorescence efficiency.

Table S2.

Amounts of Reagents Added.

Number	**1**	**2**	**3**	**4**	**5**	**6**	**7**	**……**
BSA（μL）	0	100	200	300	400	500	500	500
PBS（μL）	500	400	300	200	100	0	0	0
G250（mL）	5	5	5	5	5	5	5	5

Table S3.

Relative contents of C, N, and O in the CDs based on XPS measurement.

Sample	C (%)	N (%)	O (%)	C/O ratio
S-CDs	76.55	12.22	11.22	6.82
P-CDs	76.95	12.57	10.48	7.34
PU-CDs	60.93	13.78	25.29	2.41

Table S4.

Experimental conditions for the synthesis of CDs

Sample	**Reactant**	**Urea concentration**	**Reaction temperature**	**Time**
1	Spirulina	0	160	6
2	Phycocyanin	0	160	6
3	Phycocyanin	50	160	6
4	Phycocyanin	83.33	160	6
5	Phycocyanin	85.71	160	6
6	Phycocyanin	85.71	170	6

7	Phycocyanin	85.71	180	6
8	Phycocyanin	88.89	160	6
9	Phycocyanin	90.91	160	6
10	Phycocyanin	90.91	170	6
11	Phycocyanin	90.91	180	6
12	Phycocyanin	90.91	200	6
13	Phycocyanin	98.04	160	6
14	Phycocyanin	99.01	160	6

Table S5.

Comparison of QY enhancements among different samples

Sample	Spirulina	Crude Phycocyanin	Phycocyanin	SU-CDs	PU-CDs
QY	8.4%	14.2%	14.7%	12.7%	20.4%

Table S6.

Elemental atomic percentages of PU-CDs (Average ± Standard deviation from multiple repeated tests)

PU-CDs	C (%)	N (%)	O (%)	C/O ratio
1	60.93	13.78	25.29	2.41
2	66.96	9.0	24.00	2.79
3	68.21	10.06	21.73	3.14
Average	65.36±3.89	10.94±2.51	23.67±1.80	2.78±0.37

Table S7.

Nitrogen speciation analysis of S-CDs, P-CDs, and PU-CDs by XPS

Sample	Graphitic N	Pyridinic N
S-CDs	6.97%	93.03%
P-CDs	9.36%	90.64%
PU-CDs	69.34%	30.66%

References

1. F. S. Shan, L. J. Fu, X. Y. Chen, X. Y. Xie, C. S. Liao, Y. X. Zhu, H. Y. Xia, J. Zhang, L. Yan, Z. Y. Wang and X. Q. Yu, Chinese Chemical Letters, 2022, 33, 2942-2948.
2. J. J. Zhou, Z. H. Sheng, H. Y. Han, M. Q. Zou and C. X. Li, Mater. Lett., 2012, 66, 222-224.
3. M. Y. Fang, B. Y. Wang, X. L. Qu, S. R. Li, J. S. Huang, J. N. Li, S. Y. Lu and N. Zhou, Chinese Chemical Letters, 2024, 35, 8.
4. Y. Li, G. Bai, S. Zeng and J. Hao, ACS Applied Materials & Interfaces, 2019, 11, 4737-4744.
5. S. Thambiraj and D. R. Shankaran, Appl. Surf. Sci., 2016, 390, 435-443.
6. R. Atchudan, T. Edison, M. Shanmugam, S. Perumal, T. Somanathan and Y. R. Lee, Physica E, 2021, 126, 8.
7. X. D. Tang, H. Y. Wang, H. M. Yu, B. Bui, W. Zhang, S. Y. Wang, M. L. Chen, L. Q. Yuan, Z. Z. Hu and W. Chen, Mater. Today Phys., 2022, 22, 12.
8. J. Singh, S. Kaur, J. Lee, A. Mehta, S. Kumar, K. H. Kim, S. Basu and M. Rawat, Science of the Total Environment, 2020, 720, 8.
9. C. Z. Liang, X. B. Xie, D. D. Zhang, J. Feng, S. Y. Lu and Q. S. Shi, J. Mat. Chem. B, 2021, 9, 5670-5681.
10. T. A. Naziba, D. P. Kumar, S. Karthikeyan, S. Sriramajayam, M. Djanaguiraman, S. Sundaram, M. Ghamari, R. P. Rao, S. Ramakrishna and D. Ramesh, Chem. Rec., 2024, 24, 17.
11. 李胜慧, 何雨萱, 杜友全, 魏智鹏, 李玉 and 程倩, 发光学报, 2024, 45, 1478-1487.
12. AnyuLI, JingweiGONG, QiyanZHANG and ShuangwuHUANG, Journal of Shenzhen University Science and Engineering, 2025, 42, 146-153.
13. D. Cai, X. Zhong, L. Xu, Y. Xiong, W. Deng, G. Zou, H. Hou and X. Ji, Chem. Sci., 2025, 16, 4937-4970.
14. Q. U. Keqi, Y. O. U. Yue, C. Yang, S. H. I. Cai and H. Zhanhua, Journal of Functional Materials, 2019, 50, 9215-09220.
15. 孙英祥, 孙相宝, 何志伟, 赵增典, 刘然升 and 娄湘琴, 材料科学与工程学报, 2014, 5.
16. T. SUN, M. HU, K. LIU, Q. GAO, X. ZHENG, Y. LYU, C. XU and L. XU, Journal of Forestry Engineering, 2024, 9.
17. G. Chellasamy, S. K. Arumugasamy, S. Govindaraju and K. Yun, Chemosphere, 2022, 287, 131915.
18. 李志英 and 李洋, 化学研究与应用, 2018, 30, 6.
19. S. Li, Y. Liu, F. Huang, K. Liu and H. Chen, Chemistry and Industry of Forest Products, 2020, 40, 61-68.
20. W. QIAN, L. HE, W.-s. PAN, Y.-h. CHEN, H. WANG, S.-l. LIU, S.-j. CHEN and A.-p. LIU, Chinese Journal of Luminescence, 2021, 42, 1818-1827.
21. 程姣燕, 江西师范大学.
22. 张庆红, 孙晓峰, 阮红 and 李洪光, New Carbon Materials, 2018, 33, 571-577.
23. B. Li-Ming, D. Guo-Hua, D. Hai-Yao, L. Kun, L. Xin, W. Ting, Z. Wen-Zhi and H. Li-Juan, Chinese Journal of Applied Chemistry, 2021, 38, 202-211.

24. L. Zhu, D. Shen, Q. Wang and K. H. Luo, ACS Appl. Mater. Interfaces, 2021, 13, 56465-56475.

25. 尚永辉, 赵引涛, 陈安然, 马琳, 张红鸽 and 马思雨, 理化检验-化学分册, 2022, 58, 1189-1193.

26. 靳玉辉, 张东辉, 李媚, 林国友, 孙守祥, 孙国梁 and 方燕, 精细化工, 41.

27. 马红燕, 王靖原, 张越诚, 杨晓军 and 陈小莉, 光谱学与光谱分析, 2020, 40, 6.